Open Access Full Text Article

ORIGINAL RESEARCH

Analysis of Scheimpflug Tomography Parameters for Detecting Subclinical Keratoconus in the Fellow Eyes of Patients with Unilateral Keratoconus in the Eastern Province of Saudi Arabia

Abdulaziz Al Somali [1], Hatim Najmi[2], Hend Alsawadi[2], Hassan Alsawadi[3], Assaf AlMalki [2], Mustafa Alhamoud [2], Hatlan Alhatlan [4], Nada Alwohaibi [5]

[1]Department of Ophthalmology, King Faisal University, Alahsa, Saudi Arabia; [2]Department of Ophthalmology, Dhahran Eye Specialist Hospital, Dhahran, Saudi Arabia; [3]Department of Electrical and Computer Engineering, King Abdulaziz University, Jeddah, Saudi Arabia; [4]Department of Ophthalmology, King Fahad Hospital, Hofuf, Saudi Arabia; [5]Cornea, External Diseases, and Refractive Surgery Fellow, Dhahran Eye Specialist Hospital, Dhahran, Saudi Arabia

Correspondence: Hatim Najmi, Department of Ophthalmology, Dhahran Eye Specialist Hospital, Dhahran, Al Ameen 6927, Khobar, Eastern Province, 34446, Saudi Arabia, Tel +966533677784, Fax +966133583898, Email Hatim_najmi@hotmail.com

Purpose: We compared the characteristics of subtle morphological changes in subclinical keratoconus (KC) and normal corneas using Scheimpflug tomography (Pentacam®) and assessed the efficacy of these parameters for distinguishing KC or subclinical KC from normal eyes.

Patients and Methods: In this multicenter comparative study at Dhahran Eye Specialist Hospital and Al Kahhal Medical Complex in the Eastern Province of Saudi Arabia, we analyzed the Scheimpflug tomography charts of patients with topographically normal eyes and those with unilateral KC. Patients were divided into the normal (NL: patients considered for refractive surgery and with normal topographic/tomographic features, 129 eyes), KC (30 patients with manifest KC in one eye based on biomicroscopy and topographical findings), and forme fruste KC (FFKC: fellow eyes of patients in the KC group that met the NL group criteria) groups. Corneal morphological parameters were analyzed using the area under the receiver operating characteristic (ROC) curves (AUCs).

Results: For distinguishing NL and KC groups, all measured corneal morphological parameters, except for flat keratometry, maximum Ambrósio relational thickness index, and minimum sagittal curvature, had AUCs >0.75. The surface variance index yielded the largest AUC (0.999). For distinguishing NL and FFKC groups, all corneal morphological parameters had AUCs <0.8. Total higher-order aberrations (RMS HOA) yielded the highest AUC, followed by Belin/Ambrósio Enhanced Ectasia total deviation (BAD-D), back elevation at the thinnest location, average pachymetric progression index (PPIave), and deviation of Ambrósio relational thickness (Da) (AUC 0.74–0.78).

Conclusion: The diagnostic performance of all tested topographic and tomographic parameters measured using Scheimpflug tomography for discriminating subclinical KC was fair at best, with the top parameters being RMS HOA, BAD-D, back elevation at the thinnest location, PPIave, and Da. Distinguishing between subclinical KC and healthy eyes remains challenging. Multimodal imaging techniques may be required for optimal early detection of subtle morphological changes.

Plain language summary: Normal fellow eyes in patients with unilateral keratoconus were found to exhibit the mildest form of subclinical keratoconus. The parameters of these eyes were compared with those of normal eyes in the Saudi population using Scheimpflug tomography to detect early, subtle morphological changes. Most of the evaluated parameters were unsatisfactory in terms of their ability to discriminate between subclinical keratoconus and normal eyes, implying the need for multimodal imaging techniques for the optimal early detection of subclinical keratoconus.

Keywords: ectatic corneal disease, forme fruste keratoconus, keratoconus

Introduction

Keratoconus (KC) is a progressive noninflammatory ectatic corneal disease that usually presents in adolescence and affects both sexes and all ethnic groups. It is asymmetrical and bilateral in 90% of the cases.[1] The exact pathophysiology remains unknown. However, previous studies have linked KC to environmental and genetic factors.[1,2] Georgiou et al have found a higher incidence of KC among Asians than among Caucasians.[3] Limited studies have measured the incidence and prevalence of KC in the Saudi population.[4–6] However, the KC prevalence among Saudi pediatric patients is high, reaching 4.79%.[7] Althomali et al reported a manifest KC prevalence of up to 8.59% among Saudi adult patients seeking laser vision correction.[8]

Identifying moderate and severe forms of KC is relatively easy because of their classic clinical or topographical features. However, early diagnosis of KC with unremarkable topographic findings poses further challenges. Various terms have been used in the literature to describe the earliest KC stages, including subclinical KC, forme fruste keratoconus (FFKC), and KC suspect.[9] This overlap in terms and the resulting ambiguous definitions imply that no absolute criteria exist to distinguish early forms of KC from normal corneas. True unilateral KC has been previously indicated to be rare, and the "normal" eye is most likely to exhibit undetectable KC.[10]

Corneal topography assessment offers a revolutionary approach to diagnosing and managing KC and is considered to be a superior diagnostic method for early KC.[11] Several technologies have been developed to evaluate the corneal surface characteristics of normal corneas and those of patients with KC. These include Placido disc-based topography, slit-scanning topography, and Scheimpflug tomography.[12] In the context of identifying the early stages of KC, a Scheimpflug tomography device called the Pentacam® (Oculus, Wetzlar, Germany) was developed, which exhibited greater sensitivity across various parameters than that of Placido disc-based topography.[13–18] This device is currently considered to be a highly sensitive tool for early KC detection.[10,19] However, multiple factors, including geographic location, race, and study population size, can affect the sensitivity and specificity of the evaluated parameters.[20] To the best of our knowledge, no previous study has described changes in morphological parameters in the fellow eyes of patients with unilateral KC or compared these eyes with normal eyes in the Saudi population.

This study aimed to identify and compare the characteristics of early topographic/tomographic changes in subclinical KC and normal corneas by using Scheimpflug tomography. Furthermore, we assessed the efficacy of the evaluated parameters for distinguishing eyes with KC or subclinical KC from normal eyes.

Materials and Methods

This multicenter comparative study was conducted at Al Kahhal Medical Complex and Dhahran Eye Specialist Hospital in the Eastern Province of Saudi Arabia. We analyzed the Scheimpflug tomography charts of a cohort of topographically normal patients and a second cohort of patients with unilateral KC who visited both centers between 2018 and 2021. Patients with missing information, limited eye examinations, previous eye surgery, or ocular comorbidities that may have affected the results were excluded from the study.

The study cohort was divided into three groups. The control group consisted of patients considered for refractive surgery with myopia or myopic astigmatism and with clinically normal corneas with topographic/tomographic features falling within the normal range of parameters established by Scheimpflug tomography. The normal (NL) group consisted of patients who met the following criteria for both eyes (only one eye was randomly selected for analysis): Topographic Keratoconus Classification [TKC]=normal, typical axial topography pattern, maximum keratometry (Kmax) ≤47 D, anterior elevation at the thinnest location <15, posterior elevation at the thinnest location <18, and total higher-order aberrations (RMS HOA) <0.7 μm. Patients with manifest KC in one eye, based on biomicroscopy and/or topographical findings, exhibited the following criteria: TKC=suspicious/abnormal; axial topography pattern consistent with KC; Kmax >47.80 D; anterior elevation at the thinnest location >15; posterior elevation at the thinnest location >18; and RMS HOA >1.50 μm, while the fellow eye met the criteria of the NL group. Their affected eye was assigned to the unilateral KC group, and their fellow eye was included in the FFKC group.

All patients underwent topographic examination using a Scheimpflug Pentacam® (Oculus, Wetzlar, Germany), a tomographic device that revolves around the eye using a blue light-emitting diode at 475 nm, and a Scheimpflug camera.

Data collected included demographic data; anterior keratometric values, including flat keratometry (K1), steep keratometry (K2), mean keratometry (Km), and Kmax; front topographic astigmatism (AstigF); topometric maps indices, including the index of surface variance (ISV), index of vertical asymmetry (IVA), keratoconus index (KI), central keratoconus index (CKI), index of height asymmetry (IHA), index of height decentration (IHD), minimum sagittal curvature (Rmin), inferior-superior index (IS value), and KISA index (keratometry, IS value, skew percentage, astigmatism); topographical corneal descriptors from the Belin/Ambrósio Enhanced Ectasia Display (BAD) software in the Scheimpflug tomography device, including minimum pachymetric progression index (PPImin), average pachymetric progression index (PPIave), maximum pachymetric progression index (PPImax), maximum Ambrósio relational thickness index (ART max), deviation of normality of the front elevation (Df), deviation of normality of the back elevation (Db), deviation of normality of pachymetric progression (Dp), deviation of normality of corneal thinnest point (Dt), deviation of normality of Ambrósio relational thickness (Da), and total deviation of normality (BAD-D); front (F_Ele_Thin) and back (B_Ele_Thin) corneal elevation at the thinnest corneal location; and total higher-order aberrations (RMS HOA).

The R language (version 4.3) was used for the statistical analysis and presentation of results. The Shapiro–Wilk test was used to assess the normality of corneal morphological parameters. Measured data that followed a normal distribution are described as the mean ± standard deviation. Non-normal data are described as medians and quartile ranges. The Kruskal–Wallis test was used to compare the age, sex, and parameters of the KC, FFKC, and NL groups. Statistical significance was set at P <0.05. To investigate the differences between the two groups further, a post hoc test was conducted using Dunn's method for multiple comparisons. Given the multiple comparisons involved in pair-wise comparisons of parameters of the KC, FFKC, and NL groups, the significance level was adjusted to 0.017 following the Bonferroni principle.[21,22]

To determine the optimal cut-off values of such parameters, the sensitivity and specificity values must be closest to the area under the receiver operator characteristic (ROC) curve (AUC), and the absolute difference between the sensitivity and specificity should be minimal. The AUC is a valuable metric for comparing test results, as it reflects overall accuracy.[23,24] Thus, when distinguishing between the two diagnostic groups (FFKC and NL), the overall accuracy of an index was established using the AUC of the ROC curve.[24] The AUC was classified as excellent (>0.9), good (0.8 to 0.9), fair (0.7 to 0.8), or poor (0.6 to 0.7).[25] The DeLong test was used to assess the differences in the AUC among the various parameters. The significance level was adjusted to 0.0023 following the Bonferroni principle to account for multiple comparisons involving pair-wise comparisons of ROC curves.[21]

Ethical Considerations

The study complied with the principles of the Code of Ethics of the World Medical Association (Declaration of Helsinki). The study protocol was approved by the Bioethical Research Committee of Al Kahhal Medical Complex and Dhahran Eye Specialist Hospital. Considering the retrospective nature of this study, the requirement for obtaining informed patient consent was waived. However, the data were handled confidentially.

Results

Characteristics of Study Participants

This study included 189 eyes from 159 patients. The KC group comprised 30 eyes of 30 patients (21 men and nine women; average age, 27 ± 7 years [range, 16–47 years]), whose fellow eyes comprised the FFKC group. The NL group included 129 eyes of 129 patients (60 men and 69 women; average age, 26 ± 6 years [range, 17–48 years]). There was no significant difference in age among the KC, FFKC, and NL groups (P = 0.531). The sex distribution was significantly different among the three groups (P = 0.011).

Group Comparisons

Significant differences were observed in all morphological parameters among the three groups (P < 0.05; Table 1). All morphological parameters were significantly different between the NL and KC groups (P < 0.001). Similarly, when

Table 1 Comparison of Parameters Among the Keratoconus (KC), Forme Fruste Keratoconus (FFKC), and Normal Cornea (NL) Groups

Parameters	NL Group	KC Group	FFKC Group	(NL, KC, FFKC)	(NL vs KC)	(NL vs FFKC)	(KC vs FFKC)
	Mean /Median (Range of Variation)			P-value			
K1	42.50 (41.80–43.40)	44.70 (42.00–46.00)	42.70 (41.80–43.50)	0.004	0.001	0.574	0.025
K2	43.76 (42.34–45.18)	47.60 (44.65–51.55)	43.70 (42.27–45.14)	<0.001	<0.001	0.834	<0.001
Km	43.10 (42.40–44.00)	45.45 (43.25–48.38)	43.15 (41.83–44.48)	<0.001	<0.001	0.766	0.001
Kmax	44.20 (43.30–45.20)	53.30 (49.00–60.48)	44.54 (43.00–46.08)	<0.001	<0.001	0.283	<0.001
AstigF	1.10 (0.80–1.60)	3.30 (1.90–5.03)	0.85 (0.50–1.32)	<0.001	<0.001	0.031	<0.001
ISV	17.00 (14.00–20.00)	85.50 (54.00–138.00)	17.00 (14.25–23.00)	<0.001	<0.001	0.316	<0.001
IVA	0.11 (0.08–0.14)	0.92 (0.55–1.53)	0.14 (0.09–0.18)	<0.001	<0.001	0.008	<0.001
KI	1.02 (1.00–1.03)	1.23 (1.00–1.45)	1.02 (1.01–1.04)	<0.001	<0.001	0.029	<0.001
CKI	1.01 (1.00–1.01)	1.04 (1.02–1.10)	1.01 (1.00–1.01)	<0.001	<0.001	0.361	<0.001
IHA	5.10 (2.50–8.40)	17.40 (5.85–35.62)	5.30 (1.55–11.20)	<0.001	<0.001	0.821	<0.001
IHD	0.01 (0.01–0.01)	0.09 (0.05–0.16)	0.01 (0.01–0.01)	<0.001	<0.001	0.627	<0.001
Rmin	7.63 (7.47–7.79)	6.15 (5.09–7.21)	7.58 (7.32–7.85)	<0.001	<0.001	0.285	<0.001
IS Value	0.09 (−0.35–0.36)	6.01 (0.41–11.62)	0.44 (−0.30–1.17)	<0.001	<0.001	0.003	<0.001
KISA	4.34 (1.38–6.67)	621.62 (108.93–2859.62)	11.16 (2.61–20.73)	<0.001	<0.001	0.007	<0.001
PPImin	0.66 (0.59–0.75)	1.35 (1.06–1.95)	0.73 (0.55–0.90)	<0.001	<0.001	0.09	<0.001
PPIave	1.24 (1.05–1.43)	3.31 (2.38–4.13)	1.46 (1.20–1.72)	<0.001	<0.001	<0.001	<0.001
PPImax	0.96 (0.84–1.08)	2.18 (1.67–2.98)	1.06 (0.88–1.24)	<0.001	<0.001	0.004	<0.001
ART Max	446.00 (401.00–488.00)	145.00 (115.75–188.25)	369.00 (320.50–417.00)	<0.001	<0.001	<0.001	<0.001
Df	−0.08 (−0.55–0.42)	9.87 (4.91–12.77)	0.30 (−0.80–1.40)	<0.001	<0.001	0.182	<0.001
Db	−0.49 (−0.87–0.02)	7.63 (4.43–12.56)	−0.01 (−0.53–0.73)	<0.001	<0.001	0.001	<0.001
Dp	0.36 (−0.45–1.16)	7.77 (5.22–12.59)	1.05 (−0.15–2.25)	<0.001	<0.001	0.004	<0.001
Dt	−0.31 (−0.65–0.18)	2.04 (0.88–3.16)	0.09 (−0.35–1.06)	<0.001	<0.001	0.007	<0.001
Da	0.37 (−0.03–0.78)	3.14 (2.74–3.40)	1.05 (0.33–1.77)	<0.001	<0.001	<0.001	<0.001
BAD-D	0.80 (0.22–1.38)	8.54 (5.80–12.09)	1.57 (0.70–2.44)	<0.001	<0.001	<0.001	<0.001
F_Ele_Thin	2.00 (1.00–3.00)	21.50 (10.25–29.75)	3.03 (1.13–4.94)	<0.001	<0.001	0.03	<0.001
B_Ele_Thin	5.00 (3.00–8.00)	57.00 (30.00–74.75)	9.63 (5.24–14.03)	<0.001	<0.001	<0.001	<0.001
RMS HOA	0.38 (0.33–0.44)	3.18 (1.99–4.79)	0.50 (0.42–0.68)	<0.001	<0.001	<0.001	<0.001

Abbreviations: ART max, maximum Ambrósio relational thickness index; AstigF, front topographic astigmatism; B_Ele_Thin, back corneal elevation at the thinnest location; BAD-D, Belin/Ambrósio Enhanced Ectasia total deviation; BAD, Belin/Ambrósio Enhanced Ectasia Display; CKI, central keratoconus index; Da, deviation of normality of Ambrósio relational thickness; Db, deviation of normality of the back elevation; Df, deviation of normality of the front elevation; Dp, deviation of normality of pachymetric progression; Dt, deviation of normality of corneal thinnest point; F_Ele_Thin, front corneal elevation at the thinnest location; FFKC, forme fruste keratoconus; IHA, index of height asymmetry; IHD, index of height decentration; IS value, inferior-superior index; ISV, index of surface variance; IVA, index of vertical asymmetry; K1, flat keratometry; K2, steep keratometry; KC, keratoconus; KI, keratoconus index; KISA, keratometry, IS value, skew percentage, astigmatism index; PPIave, average pachymetric progression index; PPImax, maximum pachymetric progression index; PPImin, minimum pachymetric progression index; Rmin, minimum sagittal curvature; RMS HOA, total higher-order aberrations.

comparing the NL group with the FFKC group, significant differences were found in IVA, IS Value, ART Max, Db, Dp, Dt, Da, BAD-D, PPIave, PPI Max, B_Ele_Thin, RMS HOA, and KISA (P < 0.017).

ROC Curve Analysis of Each Parameter

The ROC curve analysis revealed that most of the measured corneal morphological parameters in the NL and KC groups had an AUC >0.75, with the exceptions of K1, ART Max, and Rmin. Notably, the ISV exhibited the highest AUC value (0.999; Table 2).

In contrast, when comparing the NL and FFKC groups, the AUCs of all corneal morphological parameters were <0.8. The RMS HOA showed the highest AUC, followed by BAD-D, B_Ele_Thin, PPIave, and Da, with AUC values ranging from 0.74 to 0.78 (Table 2 and Table 3). Figures 1 and 2 show the ROC curves for all the morphological parameters assessed.

Comparison of AUCs of Parameters

A comparison of the diagnostic capabilities of various parameters for KC and FFKC using ROC curves showed that ISV, IVA, Df, BAD-D, and B_Ele_Thin could effectively diagnose KC (AUC > 0.97). The AUCs of these parameters did not

Table 2 Receiver Operator Characteristic (ROC) Curve Analysis Results for Different Parameters in Distinguishing the Keratoconus (KC) and Forme Fruste Keratoconus (FFKC) Groups from the Normal Cornea (NL) Group

Parameters	KC Group vs NL Group				FFKC Group vs NL Group			
	AUC	Cut-off	Sensitivity	Specificity	AUC	Cut-off	Sensitivity	Specificity
K1	0.691	43.1	0.6667	0.6822	0.533	42.6	0.5333	0.5116
K2	0.826	44.7	0.7333	0.7364	0.488	43.9	0.5	0.5194
Km	0.752	43.8	0.7	0.6977	0.517	43.3	0.5333	0.5504
Kmax	0.939	46	0.9	0.907	0.563	44.7	0.5667	0.6047
AstigF	0.827	1.8	0.8	0.7907	0.374	1	0.3667	0.3876
ISV	0.999	30	0.9667	0.9767	0.559	17	0.6	0.4729
IVA	0.994	0.2	0.9333	0.938	0.656	0.13	0.6333	0.6822
KI	0.874	1.04	0.8667	0.8605	0.626	1.02	0.6333	0.4884
CKI	0.808	1.02	0.7667	0.9767	0.453	1.01	0.5333	0.3876
IHA	0.761	8.2	0.7333	0.7364	0.487	5.5	0.5	0.5039
IHD	0.961	0.019	0.9333	0.9225	0.528	0.01	0.4667	0.4884
Rmin	0.062	7.36	0.1	0.1085	0.437	7.58	0.4333	0.4341
IS value	0.902	0.75	0.8667	0.8682	0.677	0.22	0.6667	0.6512
KISA	0.949	12.067	0.9	0.907	0.659	5.092	0.5667	0.5736
PPImin	0.921	0.83	0.9	0.9147	0.600	0.7	0.5667	0.5969
PPIave	0.954	1.55	0.9333	0.907	0.741	1.34	0.7333	0.7364
PPImax	0.937	1.13	0.9	0.907	0.669	0.99	0.6	0.6202
ART max	0.053	340	0.1	0.0853	0.241	408	0.3	0.2946
Df	0.979	1.35	0.9333	0.9225	0.578	−0.04	0.5333	0.5271
Db	0.973	0.38	0.9	0.907	0.690	−0.29	0.6	0.6047
Dp	0.937	1.49	0.9	0.907	0.669	0.51	0.6333	0.6124
Dt	0.894	0.6	0.8333	0.8372	0.659	−0.17	0.6333	0.5891
Da	0.954	1.35	0.9333	0.9225	0.740	0.72	0.7	0.7054
BAD-D	0.980	1.75	0.9333	0.938	0.766	1.13	0.7	0.7054
F_Ele_Thin	0.938	5	0.9333	0.9457	0.624	3	0.5667	0.6124
B_Ele_Thin	0.983	12	0.9333	0.9612	0.766	8	0.7	0.7054
RMS HOA	0.972	0.616	0.9667	0.938	0.789	0.425	0.7	0.6977

Abbreviations: ART max, maximum Ambrósio relational thickness index; AstigF, front topographic astigmatism; B_Ele_Thin, back corneal elevation at the thinnest location; BAD-D, Belin/Ambrósio Enhanced Ectasia total deviation; BAD, Belin/Ambrósio Enhanced Ectasia Display; CKI, central keratoconus index; Da, deviation of normality of Ambrósio relational thickness; Db, deviation of normality of the back elevation; Df, deviation of normality of the front elevation; Dp, deviation of normality of pachymetric progression; Dt, deviation of normality of corneal thinnest point; F_Ele_Thin, front corneal elevation at the thinnest location; FFKC, forme fruste keratoconus; IHA, index of height asymmetry; IHD, index of height decentration; IS value, inferior-superior index; ISV, index of surface variance; IVA, index of vertical asymmetry; K1, flat keratometry; K2, steep keratometry; KC, keratoconus; KI, keratoconus index; KISA, keratometry, IS value, skew percentage, astigmatism index; Kmax, maximum keratometry; PPIave, average pachymetric progression index; PPImax, maximum pachymetric progression index; PPImin, minimum pachymetric progression index; Rmin, minimum sagittal curvature; RMS HOA, total higher-order aberrations.

Table 3 Top Five Parameters with the Highest AUC Values Distinguishing the Forme Fruste Keratoconus (FFKC) Group from the Normal Cornea (NL) Group

Parameters	FFKC Group vs NL Group			
	AUC	Cut-off	Sensitivity	Specificity
RMS HOA	0.789	0.425	0.7	0.6977
BAD-D	0.766	1.13	0.7	0.7054
B_Ele_Thin	0.766	8	0.7	0.7054
PPIave	0.741	1.34	0.7333	0.7364
Da	0.740	0.72	0.7	0.7054

Abbreviations: AUC, area under the curve; B_Ele_Thin, back corneal elevation at the thinnest location; BAD-D, Belin/Ambrósio Enhanced Ectasia total deviation; Da, deviation of normality of Ambrósio relational thickness; FFKC, forme fruste keratoconus; PPIave, average pachymetric progression index.
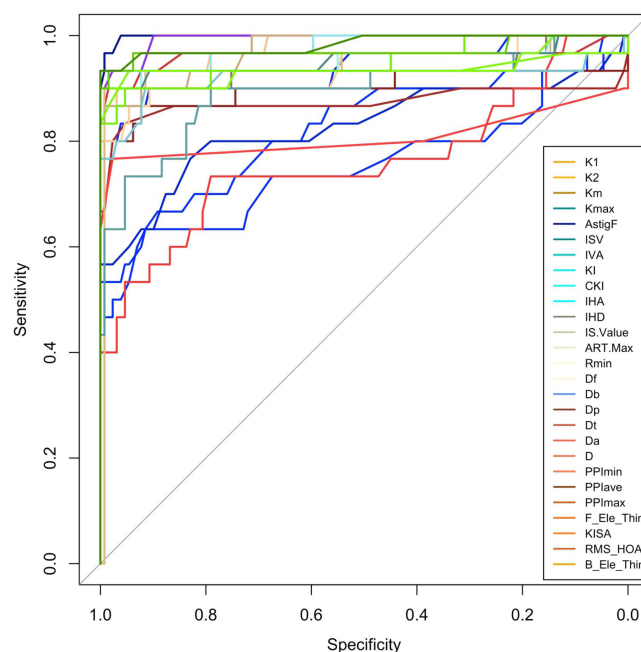
Figure 1 Receiver operating characteristic curve for distinguishing keratoconus from normal corneas.
Abbreviations: ART max, maximum Ambrósio relational thickness index; AstigF, front topographic astigmatism; B_Ele_Thin, back corneal elevation at the thinnest location; BAD-D, Belin/Ambrósio Enhanced Ectasia total deviation; CKI, central keratoconus index; Da, deviation of normality of Ambrósio relational thickness; Db, deviation of normality of the back elevation; Df, deviation of normality of the front elevation; Dp, deviation of normality of pachymetric progression; Dt, deviation of normality of corneal thinnest point; F_Ele_Thin, front corneal elevation at the thinnest location; IHA, index of height asymmetry; IHD, index of height decentration; IS value, inferior-superior index; ISV, index of surface variance; IVA, index of vertical asymmetry; K1, flat keratometry; K2, steep keratometry; KC, keratoconus; KI, keratoconus index; KISA, keratometry, IS value, skew percentage, astigmatism index; Km, mean keratometry; Kmax, maximum keratometry; PPIave, average pachymetric progression index; PPImax, maximum pachymetric progression index; PPImin, minimum pachymetric progression index; Rmin, minimum sagittal curvature; RMS HOA, total higher-order aberrations.
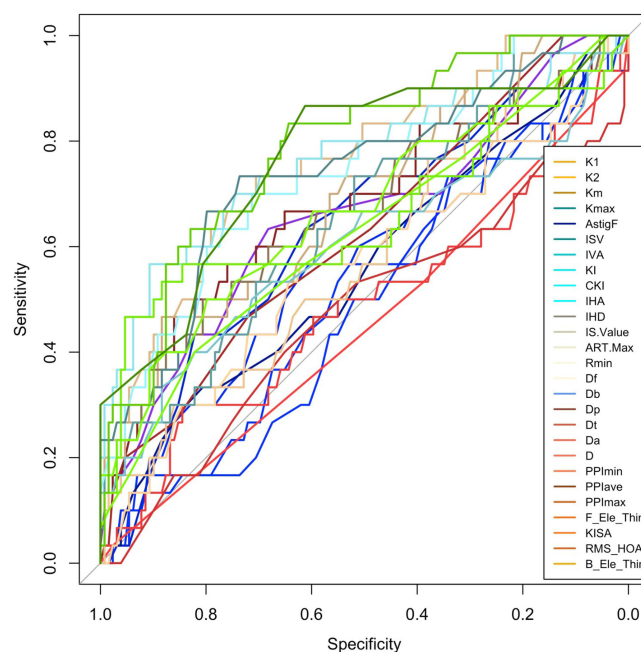

Figure 2 Receiver operating characteristic curve for distinguishing forme fruste keratoconus from normal corneas.
Abbreviations: ART max, maximum Ambrósio relational thickness index; AstigF, front topographic astigmatism; B_Ele_Thin, back corneal elevation at the thinnest location; BAD-D, Belin/Ambrósio Enhanced Ectasia total deviation; CKI, central keratoconus index; Da, deviation of normality of Ambrósio relational thickness; Db, deviation of normality of the back elevation; Df, deviation of normality of the front elevation; Dp, deviation of normality of pachymetric progression; Dt, deviation of normality of corneal thinnest point; F_Ele_Thin, front corneal elevation at the thinnest location; IHA, index of height asymmetry; IHD, index of height decentration; IS value, inferior-superior index; ISV, index of surface variance; IVA, index of vertical asymmetry; K1, flat keratometry; K2, steep keratometry; KC, keratoconus; KI, keratoconus index; KISA, keratometry, IS value, skew percentage, astigmatism index; Km, mean keratometry; Kmax, maximum keratometry; PPIave, average pachymetric progression index; PPImax, maximum pachymetric progression index; PPImin, minimum pachymetric progression index; Rmin, minimum sagittal curvature; RMS HOA, total higher-order aberrations.

Table 4 Comparison of the Receiver Operator Characteristic (ROC) Curves of Some Parameters in the Keratoconus (KC), Forme Fruste Keratoconus (FFKC), and the Normal Cornea (NL) Groups

Parametric Curves Compared		P-value (KC vs NL)	P-value (FFKC vs NL)
ISV	IVA	0.191	0.047
	Df	0.113	0.751
	Da	0.149	0.006
	BAD-D	0.183	<0.001
	RMS HOA	0.297	<0.001
	B_Ele_Thin	0.273	0.001
IVA	Df	0.267	0.131
	Da	0.157	0.233
	BAD-D	0.223	0.076
	PPIave	0.16	0.245
	RMS HOA	0.339	0.028
	B_Ele_Thin	0.399	0.08
Df	Da	0.478	0.019
	BAD-D	0.958	<0.001
	PPIave	0.48	0.023
	RMS HOA	0.81	0.003
	B_Ele_Thin	0.81	0.002
Da	BAD-D	0.131	0.449
	PPIave	1	0.945
	RMS HOA	0.543	0.455
	B_Ele_Thin	0.119	0.645
BAD-D	PPIave	0.135	0.531
	RMS HOA	0.725	0.743
	B_Ele_Thin	0.507	0.998
PPIave	RMS HOA	0.554	0.472
	B_Ele_Thin	0.117	0.646
RMS HOA	B_Ele_Thin	0.671	0.766

Abbreviations: B_Ele_Thin, back corneal elevation at the thinnest location; BAD-D, Belin/Ambrósio Enhanced Ectasia total deviation; Da, deviation of normality of Ambrósio relational thickness; Df, deviation of normality of the front elevation; FFKC, forme fruste keratoconus; ISV, index of surface variance; IVA, index of vertical asymmetry; PPIave, average pachymetric progression index; RMS HOA, total higher-order aberrations.

show any statistically significant differences in terms of KC diagnostic ability, although ISV and IVA exhibited greater AUCs, suggesting greater efficiency in diagnosing KC than that of the other parameters (Table 4).

On the other hand, RMS HOA, BAD-D, B_Ele_Thin, PPIave, and Da could effectively diagnose FFKC (AUC > 0.70). The AUCs of these tested parameters showed no statistically significant differences in any pair-wise comparison. However, RMS HOA, B_Ele_Thin, and BAD-D demonstrated higher AUCs than the other parameters, indicating that they may have greater efficiency in diagnosing FFKC (Table 4).

Discussion

In this study, we aimed to identify subtle changes in the morphological parameters of subclinical KC, compare them with those in normal corneas, and validate the ability of different Scheimpflug tomography parameters and their optimized cut-off values to detect subclinical KC in a considerably large sample of patients in Saudi Arabia. Most of the tested parameters could differentiate NL from KC with an AUC >0.75, except for K1, ARTMax, and Rmin. The ISV yielded the largest AUC (0.999), followed by the IVA, B-Ele-Thin, and BAD-D (Table 2). These results corroborated findings from

previous studies that Scheimpflug tomography can accurately distinguish eyes with KC from normal eyes.[11,13,23,26] However, our findings also indicated that individual parameters derived from Scheimpflug tomography were suboptimal in distinguishing between normal eyes and eyes with subclinical KC. ROC curve analysis of the NL and FFKC groups showed AUCs <0.8 for all corneal morphological parameters. Among all parameters, RMS HOA was found to have the highest AUC, consistent with other similar studies.[27–29] Following RMS HOA, the BAD-D index also showed noteworthy diagnostic performance. Back elevation at the thinnest location, PPIave, and Da exhibited relatively high AUC values (range: 0.74–0.78), which implies a 74–78% likelihood of accurately classifying cases as having subclinical KC based on these parameters. Therefore, we suggest careful examination of these parameters with their effective cut-off values (Table 3) as screening tools that may help to exclude patients from laser vision correction and prevent post-refractive surgery ectasia in our population, particularly in cases where the anterior axial curvature is normal and posterior elevation is <18 μm.

According to the 2015 consensus of the Global Consensus on Keratoconus and Ectatic Diseases panel, tomography (such as Scheimpflug or optical coherence tomography) is the most reliable and readily available test for diagnosing early KC, and the presence of posterior corneal elevation abnormalities is necessary to determine mild or subclinical KC.[30] However, the available literature on the diagnostic value of posterior elevation in the detection of subclinical KC is limited.

Our study is one of the few to date that has included tomography as a parameter for detecting subclinical KC. Despite being one of the best parameters for detecting KC, posterior elevation at the thinnest location was not superior to accurately distinguishing subclinical KC. These findings were consistent with those of most other studies that investigated posterior elevation.[13,23,31] Vasquez et al concluded that the posterior corneal surface deviation index failed to detect subclinical KC. It was not superior to anterior corneal surface deviation, as it only detected approximately 50% of subclinical KC eyes.[23] Hwang et al studied tomographic variables from Scheimpflug and spectral-domain optical coherence tomography (SD-OCT) and concluded that combining variables effectively detected subclinical KC. Interestingly, the accuracy of their model decreased with the addition of posterior elevation data.[31] In contrast, De Sanctis et al reported a high overall accuracy of posterior elevation but found that it did not perform as well in distinguishing subclinical KC from KC. A posterior elevation of >29 μm could be used to detect subclinical KC with a high degree of specificity (90.8%) but low sensitivity (68%).[14] However, notably, the diagnostic criteria established by De Sanctis et al[14] for defining subclinical KC were less rigid than those used in our study and in other studies with similar findings.[13,23,31] This difference in criteria may account for the observed contradiction. Considering the available data, posterior elevation obtained using the Scheimpflug technology may not be necessary to diagnose subclinical KC.

Elevation maps of Scheimpflug tomography were generated by comparing the reconstructed anterior and posterior surfaces with the best-fitted surface, with a standard reference size of 8 mm. Thus, the corneal apex can be elevated anteriorly and posteriorly at the minimum thickness.[32] As Scheimpflug tomography measures anterior and posterior surface elevations, it applies a best-fit surface to both surfaces; however, the apical protrusion can steepen the best-fit surface, resulting in a further negligible difference. The BAD in the Scheimpflug tomography system solves this problem by eliminating the 3–4-mm area of the thinnest pachymetry and creating an enhanced best-fit sphere.[32] Hashemi et al reported that BAD-D on Scheimpflug tomography was the strongest factor for diagnosing subclinical and clinical KC. A combination of BAD-D, vertical coma aberration, IVA, and ISV could be used to detect subclinical KC when the corneal curvature patterns are normal.[33] Shetty et al reported similar findings, concluding that BAD-D was the best marker for differentiating KC and subclinical KC from normal corneas.[11] In our study, this was not the case, as the BAD-D demonstrated poor performance in detecting subclinical KC, which was consistent with the findings of Bae et al.[13] Our study's stricter inclusion criteria for defining fellow eyes may account for this inconsistency.

Even though the topographic and tomographic indices derived by Scheimpflug tomography are excellent at distinguishing manifest KC from normal eyes, no individual parameter was capable of detecting subclinical KC, as previously described.[31] Some reports have indicated that the epithelial thickness standard deviation (pattern standard deviation) is a strong predictor of early KC,[34] whereas others have indicated epithelial thickness at the thinnest point to be useful for diagnosing early subclinical KC.[35]

The retrospective nature of our study and the lack of long-term follow-up may have limited our ability to identify the progression risk and accuracy of the parameters. Identifying parameters for early KC diagnosis is crucial. Further research with similar strict inclusion criteria and longer follow-up periods, focusing on corneal biomechanics, wavefront aberrations, SD-OCT, and epithelial mapping, is required.

Conclusion

Distinguishing between eyes with subclinical KC and healthy eyes remains a challenge. Herein, the diagnostic performance of all tested topographic and tomographic parameters using Scheimpflug tomography to discriminate subclinical KC was fair at best, with the top parameters being RMS HOA, BAD-D, back elevation at the thinnest location, PPIave, and Da. Thus, multimodal imaging techniques for optimal early detection of subtle morphological changes may be required.

Abbreviations

ART max, maximum Ambrósio relational thickness index; AstigF, front topographic astigmatism; AUC, area under the curve; B_Ele_Thin, back corneal elevation at the thinnest location; BAD, Belin/Ambrósio Enhanced Ectasia Display; BAD-D, Belin/Ambrôsio Enhanced Ectasia Total Deviation; CKI, central keratoconus index; Da, deviation of normality of Ambrôsio relational thickness; Db, deviation of normality of the back elevation; Df, deviation of normality of the front elevation; Dp, deviation of normality of pachymetric progression; Dt, deviation of normality of corneal thinnest point; F_Ele_Thin, front corneal elevation at the thinnest location; FFKC, forme fruste keratoconus; IHA, index of height asymmetry; IHD, index of height decentration; IS value, inferior-superior index; ISV, index of surface variance; IVA, index of vertical asymmetry; K1, flat keratometry; K2, steep keratometry; KC, keratoconus; KI, keratoconus index; KISA, keratometry, IS value, skew percentage, astigmatism index; Km, mean keratometry; Kmax, maximum keratometry; PPIave, average pachymetric progression index; PPImax, maximum pachymetric progression index; PPImin, minimum pachymetric progression index; Rmin, minimum sagittal curvature; RMS HOA, total higher-order aberrations; ROC, receiver operating characteristic; SD-OCT, spectral-domain optical coherence tomography.

Data Sharing Statement

All data generated or analyzed during this study are included in this article. Further inquiries can be directed to the corresponding author.

Ethics Approval and Informed Consent

The study complied with the principles of the Code of Ethics of the World Medical Association (Declaration of Helsinki). The study protocol was approved by the Bioethical Research Committee of Al Kahhal Medical Complex and Dhahran Eye Specialist Hospital. Considering the retrospective nature of this study, the requirement for informed consent was waived.

Author Contributions

All authors made a significant contribution to the work reported, whether that is in the conception, study design, execution, acquisition of data, analysis, and interpretation, or in all these areas; took part in drafting, revising, or critically reviewing the article; gave final approval of the version to be published; have agreed on the journal to which the article has been submitted; and agree to be accountable for all aspects of the work.

Funding

This project received no specific grants from any funding agencies.

Disclosure

The authors report no conflicts of interest in this work.

References

1. Mas Tur V, MacGregor C, Jayaswal R, O'Brart D, Maycock N. A review of keratoconus: diagnosis, pathophysiology, and genetics. *Surv Ophthalmol*. 2017;62(6):770–783. doi:10.1016/j.survophthal.2017.06.009

2. Moussa S, Grabner G, Ruckhofer J, Dietrich M, Reitsamer H. Genetics in keratoconus – what is new? *Open Ophthalmol J*. 2017;11:201–210. doi:10.2174/1874364101711010201

3. Georgiou T, Funnell CL, Cassels-Brown A, O'Conor R. Influence of ethnic origin on the incidence of keratoconus and associated atopic disease in Asians and white patients. *Eye*. 2004;18(4):379–383. doi:10.1038/sj.eye.6700652

4. Alabdelmoneam M. Retrospective analysis of keratoconus at King Khaled Eye Specialist Hospital, Riyadh, Saudi Arabia. *Clin Optom*. 2012;4:7–12. doi:10.2147/OPTO.S28461

5. Assiri AA, Yousuf BI, Quantock AJ, Murphy PJ. Incidence and severity of keratoconus in Asir province, Saudi Arabia. *Br J Ophthalmol*. 2005;89(11):1403–1406. doi:10.1136/bjo.2005.074955

6. Alzahrani K, Al-Rashah A, Al-Salem S, et al. Keratoconus epidemiology presentations at Najran Province, Saudi Arabia. *Clin Optom*. 2021;13:175–179. doi:10.2147/OPTO.S309651

7. Torres Netto EA, Al-Otaibi WM, Hafezi NL, et al. Prevalence of keratoconus in paediatric patients in Riyadh, Saudi Arabia. *Br J Ophthalmol*. 2018;102(10):1436–1441. doi:10.1136/bjophthalmol-2017-311391

8. Althomali TA, Al-Qurashi IM, Al-Thagafi SM, Mohammed A, Almalki M. Prevalence of keratoconus among patients seeking laser vision correction in Taif area of Saudi Arabia. *Saudi J Ophthalmol*. 2018;32(2):114–118. doi:10.1016/j.sjopt.2017.11.003

9. Shi Y. Strategies for improving the early diagnosis of keratoconus. *Clin Optom*. 2016;8:13–21. doi:10.2147/OPTO.S63486

10. Li X, Rabinowitz YS, Rasheed K, Yang H. Longitudinal study of the normal eyes in unilateral keratoconus patients. *Ophthalmology*. 2004;111(3):440–446. doi:10.1016/j.ophtha.2003.06.020

11. Shetty R, Rao H, Khamar P, et al. Keratoconus screening indices and their diagnostic ability to distinguish normal from ectatic corneas. *Am J Ophthalmol*. 2017;181:140–148. doi:10.1016/j.ajo.2017.06.031

12. Shetty R, Arora V, Jayadev C, et al. Repeatability and agreement of three Scheimpflug-based imaging systems for measuring anterior segment parameters in keratoconus. *Invest Ophthalmol Vis Sci*. 2014;55(8):5263–5268. doi:10.1167/iovs.14-15055

13. Bae GH, Kim JR, Kim CH, Lim DH, Chung ES, Chung TY. Corneal topographic and tomographic analysis of fellow eyes in unilateral keratoconus patients using pentacam. *Am J Ophthalmol*. 2014;157(1):103–109.e1. doi:10.1016/j.ajo.2013.08.014

14. de Sanctis U, Loiacono C, Richiardi L, Turco D, Mutani B, Grignolo FM. Sensitivity and specificity of posterior corneal elevation measured by Pentacam in discriminating keratoconus/subclinical keratoconus. *Ophthalmology*. 2008;115(9):1534–1539. doi:10.1016/j.ophtha.2008.02.020

15. Piñero DP, Alió JL, Alesón A, Escaf Vergara M, Miranda M. Corneal volume, pachymetry, and correlation of anterior and posterior corneal shape in subclinical and different stages of clinical keratoconus. *J Cataract Refract Surg*. 2010;36(5):814–825. doi:10.1016/j.jcrs.2009.11.012

16. Ambrósio R, Alonso RS, Luz A, Coca Velarde LG. Corneal-thickness spatial profile and corneal-volume distribution: tomographic indices to detect keratoconus. *J Cataract Refract Surg*. 2006;32(11):1851–1859. doi:10.1016/j.jcrs.2006.06.025

17. Ambrósio R, Caiado AL, Guerra FP, et al. Novel pachymetric parameters based on corneal tomography for diagnosing keratoconus. *J Refract Surg*. 2011;27(10):753–758. doi:10.3928/1081597X-20110721-01

18. Ambrósio R, Nogueira LP, Caldas DL, et al. Evaluation of corneal shape and biomechanics before LASIK. *Int Ophthalmol Clin*. 2011;51(2):11–38. doi:10.1097/IIO.0b013e31820f1d2d

19. McAlinden C, Khadka J, Pesudovs K. A comprehensive evaluation of the precision (repeatability and reproducibility) of the oculus Pentacam HR. *Invest Ophthalmol Vis Sci*. 2011;52(10):7731–7737. doi:10.1167/iovs.10-7093

20. Huseynli S, Abdulaliyeva F. Evaluation of scheimpflug tomography parameters in subclinical keratoconus, clinical keratoconus and normal Caucasian eyes. *Turk J Ophthalmol*. 2018;48(3):99–108. doi:10.4274/tjo.89587

21. Bitnun A. Etymologia: Bonferroni Correction. *Emerg Infect Dis*. 2015;21(2):289. doi:10.3201/eid2102.et2102

22. Guo LL, Tian L, Cao K, et al. Comparison of the morphological and biomechanical characteristics of keratoconus, forme fruste keratoconus, and normal corneas. *Semin Ophthalmol*. 2021;36(8):671–678. doi:10.1080/08820538.2021.1896752

23. Ruiseñor Vázquez PR, Galletti JD, Mínguez N, et al. Pentacam Scheimpflug tomography findings in topographically normal patients and subclinical keratoconus cases. *Am J Ophthalmol*. 2014;158(1):32–40.e2. doi:10.1016/j.ajo.2014.03.018

24. Florkowski CM. Sensitivity, specificity, receiver-operating characteristic (ROC) curves and likelihood ratios: communicating the performance of diagnostic tests. *Clin Biochem Rev*. 2008;29(Suppl 1):S83.

25. Motlagh MN, Moshirfar M, Murri MS, et al. Pentacam® corneal tomography for screening of refractive surgery candidates: a review of the literature, Part I. *Med Hypothesis Discov Innov Ophthalmol*. 2019;8(3):177–203.

26. Huseynli S, Salgado-Borges J, Alio JL. Comparative evaluation of Scheimpflug tomography parameters between thin non-keratoconic, subclinical keratoconic, and mild keratoconic corneas. *Eur J Ophthalmol*. 2018;28(5):521–534. doi:10.1177/1120672118760146

27. Kandel S, Chaudhary M, Mishra SK, et al. Evaluation of corneal topography, pachymetry and higher order aberrations for detecting subclinical keratoconus. *Ophthalmic Physiol Opt*. 2022;42(3):594–608. doi:10.1111/opo.12956

28. Koh S, Inoue R, Maeno S, et al. Characteristics of higher-order aberrations in different stages of keratoconus. *Eye Contact Lens*. 2022;48(6):256–260. doi:10.1097/ICL.0000000000000897

29. Salman A, Kailani O, Marshall J, et al. Evaluation of anterior and posterior corneal higher order aberrations for the detection of keratoconus and suspect keratoconus. *Tomography*. 2022;8(6):2864–2873. doi:10.3390/tomography8060240

30. Gomes JA, Tan D, Rapuano CJ, et al. Global consensus on keratoconus and ectatic diseases. *Cornea*. 2015;34(4):359–369. doi:10.1097/ICO.0000000000000408

31. Hwang ES, Perez-Straziota CE, Kim SW, Santhiago MR, Randleman JB. Distinguishing highly asymmetric keratoconus eyes using combined Scheimpflug and spectral-domain OCT analysis. *Ophthalmology*. 2018;125(12):1862–1871. doi:10.1016/j.ophtha.2018.06.020

32. Cavas-Martínez F, De la Cruz Sánchez E, Nieto Martínez J, Fernández Cañavate FJ, Fernández-Pacheco DG. Corneal topography in keratoconus: state of the art. *Eye Vis*. 2016;3(1):5. doi:10.1186/s40662-016-0036-8

33. Hashemi H, Beiranvand A, Yekta A, Maleki A, Yazdani N, Khabazkhoob M. Pentacam top indices for diagnosing subclinical and definite keratoconus. *J Curr Ophthalmol*. 2016;28(1):21–26. doi:10.1016/j.joco.2016.01.009

34. Li Y, Chamberlain W, Tan O, Brass R, Weiss JL, Huang D. Subclinical keratoconus detection by pattern analysis of corneal and epithelial thickness maps with optical coherence tomography. *J Cataract Refract Surg*. 2016;42(2):284–295. doi:10.1016/j.jcrs.2015.09.021

35. Temstet C, Sandali O, Bouheraoua N, et al. Corneal epithelial thickness mapping using Fourier-domain optical coherence tomography for detection of form fruste keratoconus. *J Cataract Refract Surg*. 2015;41(4):812–820. doi:10.1016/j.jcrs.2014.06.043